



Influence of temperature variation on field effect transistor properties using a solution-processed liquid crystalline semiconductor, C₈BTBT

Hirosato Monobe, Masaomi Kimoto & Yo Shimizu

To cite this article: Hirosato Monobe, Masaomi Kimoto & Yo Shimizu (2016) Influence of temperature variation on field effect transistor properties using a solution-processed liquid crystalline semiconductor, C₈BTBT, *Molecular Crystals and Liquid Crystals*, 629:1, 181-186, DOI: 10.1080/15421406.2015.1094610

To link to this article: <http://dx.doi.org/10.1080/15421406.2015.1094610>



Published online: 16 Jun 2016.



Submit your article to this journal [↗](#)



Article views: 61



View related articles [↗](#)



View Crossmark data [↗](#)

Influence of temperature variation on field effect transistor properties using a solution-processed liquid crystalline semiconductor, C₈BTBT

Hirosato Monobe^a, Masaomi Kimoto^b, and Yo Shimizu^a

^aResearch Institute for Ubiquitous Energy Devices, National Institute of Advanced Industrial Science and Technology (AIST), Midorigaoka, Ikeda, Osaka, Japan; ^bOkuno Chemical Industries Co., Ltd., Jyoutou-ku, Osaka, Japan

ABSTRACT

In this study, we used a LC semiconductor, C₈BTBT, solution (e.g. 0.1 wt % in heptane) for forming an organic semiconductor layer by casting method, and fabricated bottom-gate/bottom-contact type FETs. The FETs mobility was determined 0.17 cm² V⁻¹ s⁻¹ which was comparable to that determined by time-of-flight technique in a sandwich type cell at room temperature. We have investigated the surface morphology and the influence of temperature variation on FET properties. The LC FET mobility was kept below 60°C and drastically decreased after heat stress above 100°C irreversibly.



KEYWORDS

Liquid crystals; liquid crystalline semiconductor; field effect transistor; temperature variation; printed electronics

1. Introduction

In the field of organic electronics, solution-processed organic semiconductors for large and flexible electronic devices which are fabricated by low temperature process, in particular field effect transistors (FETs) have gotten much attention in these years [1, 2]. Numerous of the characteristic properties of liquid crystalline (LC) semiconductors, such as good solubility in ordinary organic solvents, their self-assembling nature, electrically inactive domain boundaries, and uniformity of obtained film, make them attractive candidates for application in FET devices [3–9]. Especially, a rod-like liquid crystal, dialkyl-benzothienobenzothiophene (C_nBTBT) is widely studied as a LC semiconductor in FET applications, and its mobility has been achieved over 1~10 cm² V⁻¹ s⁻¹ in solution-processed FETs at room temperature [10–24]. Its dioctyl-substituted derivative, 2,7-dioctyl[1]benzothieno[3,2-*b*][1]benzothiophen (C₈BTBT) shows a smectic A (SmA) mesophase which consists a layered structure and its melting and clearing points are 110°C and 126°C, respectively [25].

In this study, we used a LC semiconductor, C₈BTBT, solution (e.g. 0.1 wt % in n-heptane) for forming an organic semiconductor layer by casting method, and fabricated bottom-gate/bottom-contact (BGBC) type FETs. We have investigated the surface morphology and the influence of temperature variation on FET properties across the phase transition from

CONTACT Hirosato Monobe  monobe-hirosato@aist.go.jp  Research Institute for Ubiquitous Energy Devices, National Institute of Advanced Industrial Science and Technology (AIST), Midorigaoka, Ikeda, Osaka 563-8577, Japan
This paper was originally submitted to *Molecular Crystals and Liquid Crystals*, Volumes 620–622, Proceedings of the KJF International Conference on Organic Materials for Electronics and Photonics 2014.

crystal to mesophase. The FETs mobility was compared with that determined by time-of-flight (TOF) technique which was obtained for a sandwich type cell.

2. Experimental methods

A LC semiconductor, C₈BTBT, was purchased from Luminescence Technology and used after purification by column chromatography and recrystallization from hexane.

The drift charge carrier mobility was measured by TOF technique for a LC film sandwiched between Indium-Tin-Oxide covered glass plates. The cell was capillary filled in under Ar gas after being degassed under vacuum by slowly cooling the sample from the isotropic liquid state. No surface treatment was used in this study. The cell was set up in a hot stage equipped with a polarizing microscope and externally biased by dry battery cells. A N₂ laser ($\lambda = 337\text{nm}$, 800 ps, $\varphi = 1\text{ mm}$) was used for a pulsed light irradiation. A transient photocurrent was detected by a digital oscilloscope (Agilent, HP54820A) with a high-speed current amplifier (FEMTO, DHPCA-100).

For the FET devices, an organic semiconductor film was deposited by solution casting method onto the non-pretreated thermally oxidized, highly n-doped silicon substrates from a 0.1 wt % C₈BTBT n-heptane solution with inclined configuration and dried under the atmosphere at room temperature. FET devices were fabricated in BGBC geometry with a 300 nm-thick SiO₂ gate dielectric. Gold source and drain electrodes with 50 nm-thick were evaporated on a 3-nm-thick co-deposited adhesive layer consists of gold and nickel (9:1) through shadow masks under 5×10^{-4} Pa, producing the channel length/width (L/W) of 56/2000 μm . The electrodes were chemically modified with pentafluorobenzenethiol (PFBT) by immersing into 10 mM its ethanol solution at 30 minutes to improve potential matching between electrodes and an organic semiconductor [26]. The chemical structure of C₈BTBT and the device geometry of FET are shown in Figure 1.

A film structure of LC semiconductor layer of FETs was investigated by optical microscopy (OM) and atomic force microscopy (AFM) (SII, SPA350). All FET measurements were carried out under Ar atmosphere using a sourcemeter (Keithley, 2636A) and a temperature controlled stage. FET mobility (μ_{FET}) was calculated in the saturation regime by using the relationship: $\mu_{\text{FET}} = (2I_{\text{ds}}^{\text{sat}}L) / (WC(V_{\text{g}} - V_{\text{th}})^2)$, where $I_{\text{ds}}^{\text{sat}}$ is the source-drain saturation current, C is the dielectric capacitance, V_{g} is the gate voltage, and V_{th} is the threshold voltage. The latter can be estimated as the intercept of the linear section of the plot of V_{G} vs. $(I_{\text{ds}})^{1/2}$ (at $V_{\text{ds}} = -50\text{ V}$).

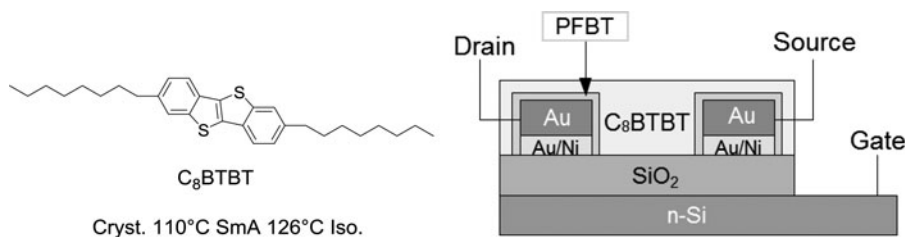


Figure 1. Chemical structure and phase transition temperature of C₈BTBT and schematic representation of the BGBC FET device configuration.

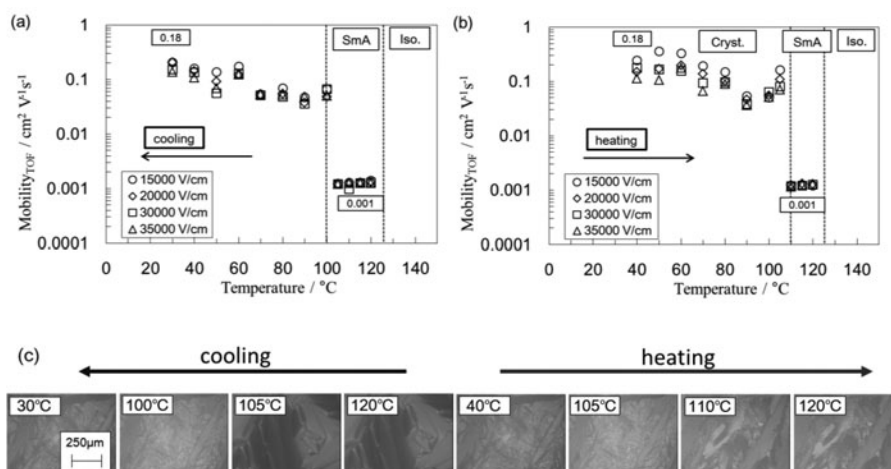


Figure 2. Temperature dependence of drift charge carrier mobility of C_8BTBT for positive carriers (hole) on (a) cooling and (b) heating process. (c) a series of polarized microscopic images of the sample cell at various temperatures.

3. Results and discussion

3.1. Temperature dependence of TOF mobility

The temperature dependence of drift mobility was performed by TOF technique for C_8BTBT in a sandwich type ITO cell (thickness 19.0 μm). Figures 2(a) and 2(b) show temperature dependence of the charge carrier mobility on cooling and heating processes, respectively. The drift mobility of hole is in the range of 0.08 ~ 0.18 and 0.001 $cm^2 V^{-1} s^{-1}$ in the crystal and SmA phases, respectively. Figure 2(c) shows a series of polarized microscopic images of the sample cell at various temperatures. A typical fan-shaped texture was seen for SmA mesophase. Almost same texture with cracks at domain boundaries was shown after the phase transition to the crystal phase with temperature decreases, indicating a layered structure in which molecules lied down on the substrate was remained. Cracks at domain boundaries are disappeared with the phase transition to SmA mesophase on re-heating process in a sandwich type cell. This implies the self-healing effect at the domain boundaries exists in a film confined between two ITO plates. The drift mobility determined by TOF technique shows reversible change on temperature variation without electric field dependency in a sandwich type cell.

3.2. FET characteristics and film morphology

Figure 3 shows the typical transfer and output characteristics of the solution casted C_8BTBT film of BGBC type FETs. FET mobility was calculated to be 0.17 $cm^2 V^{-1} s^{-1}$, whereas drift mobility determined by TOF technique was 0.18 $cm^2 V^{-1} s^{-1}$ at room temperature. The mobility of FETs is rather smaller than that reported previously [11–16, 21–24], this might arises from the poor quality of organic semiconductor film in this experiment and the charge injection resistance of BGBC type devices [27].

Figure 4 shows the OM and AFM images of FET devices at room temperature and those after temperature variation measurements up to 110°C which is the melting point of C_8BTBT . A fine terrace structure was clearly observed for a C_8BTBT film which consists of a molecular layered structure before heat stress. On the other hand, no film structure was seen on the

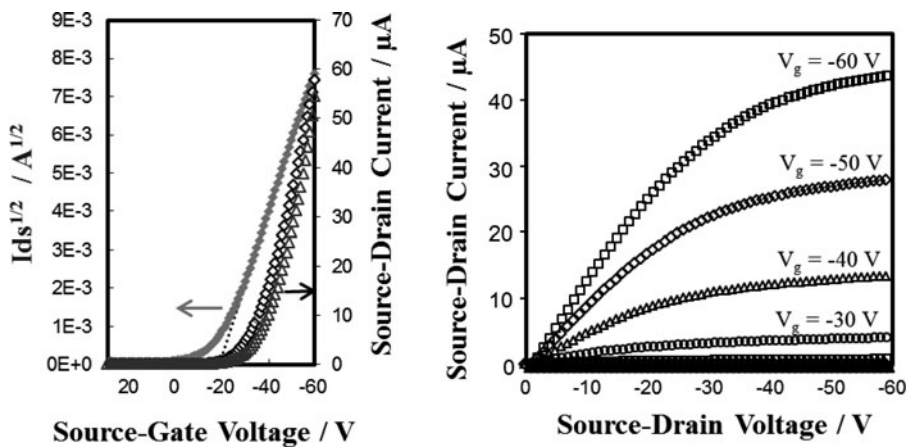


Figure 3. (a) Typical output and (b) transfer characteristic curves of solution casted C_6 BTBT film of BGBC FETs.

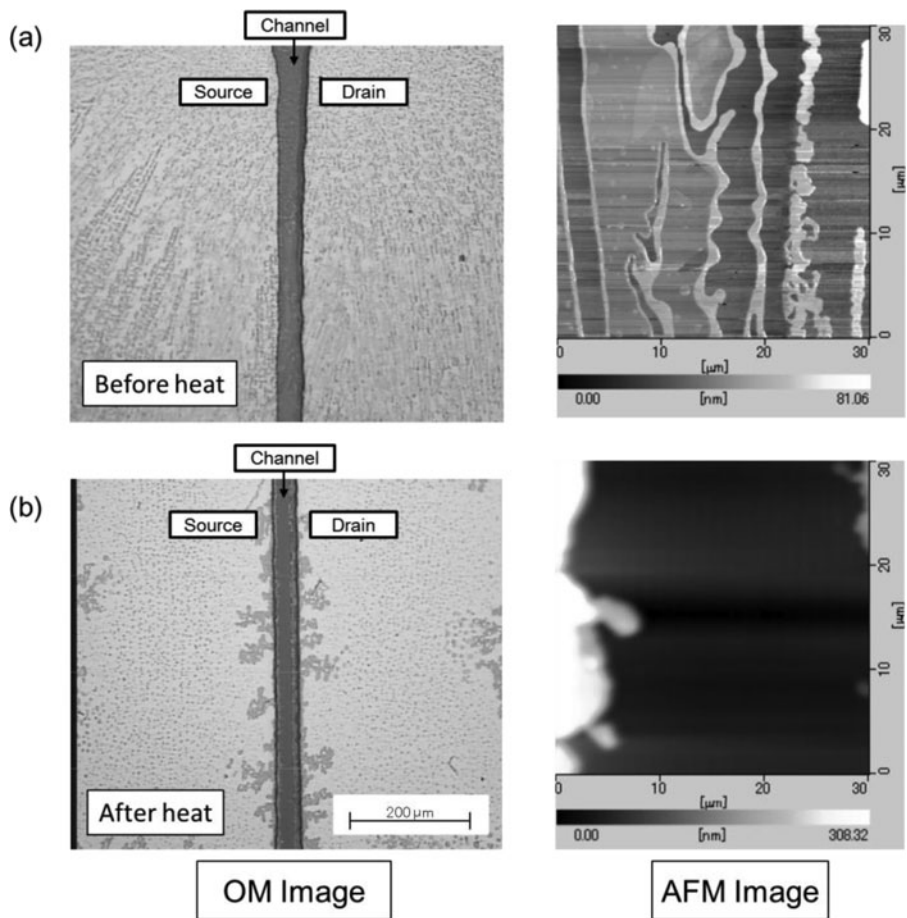


Figure 4. OM and AFM images of a C_6 BTBT FET device between source and drain electrodes (a) before heating and (b) after FET measurement on 110°C heating at room temperature.

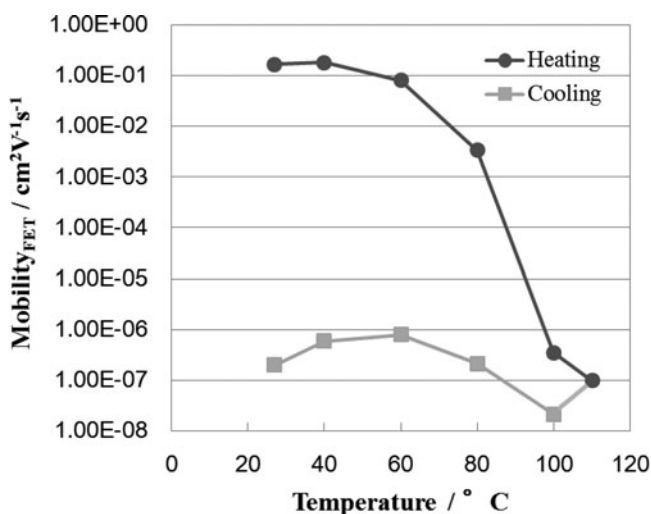


Figure 5. Temperature dependence of FET mobility of C₈BTBT on heating (circle) and cooling (square) process.

channel area between source and drain electrodes of the FET device after heat stress, implying a semiconductor material moved away due to the aggregation at fluid state in the SmA mesophase.

Figure 5 shows the temperature dependence of FET mobility of BGBC FETs. FET mobility was calculated to be $0.17 \text{ cm}^2 \text{ V}^{-1} \text{ s}^{-1}$ at room temperature to 60°C , where it decreased in the order of $10^{-3} \text{ cm}^2 \text{ V}^{-1} \text{ s}^{-1}$ at 80°C followed by drastically decreased less than $10^{-6} \text{ cm}^2 \text{ V}^{-1} \text{ s}^{-1}$ at above 100°C which is near the melting point of C₈BTBT. The FET mobility does not recover after the phase transition from SmA to crystal phases on cooling process. Irreversible change of FET mobility could be accountable to the irreversible morphological change of the semiconductor layer on the channel area due to the material movement in fluid LC phase without topological confinement in an open film configuration, which is consistent with the OM and AFM observation. It might be possible to obtain reversible change of FET mobility with temperature variation, if a semiconductor film used with a proper confined topological configuration such as an over-coating protect layer in the same manner as the TOF sandwich type cell although the alignment direction of LC layer normal is different each other.

4. Conclusions

We fabricated FETs of BGBC geometry by solution casting from a LC semiconductor, C₈BTBT, solution (e.g. 0.1 wt % in n-heptane). The solution-processed BGBC FETs show FET characteristics and mobility was $0.17 \text{ cm}^2 \text{ V}^{-1} \text{ s}^{-1}$ which was comparable to that determined by time-of-flight technique at room temperature. The FET mobility was kept on until 60°C and following irreversible decrease after temperature heat stress above 100°C which is near the phase transition temperature from crystal to SmA mesophase. For the practical use, the improvement of thermal stability of LC materials would be required for FET applications [20].

References

- [1] Dimitrakopoulos, C. D., & Malenfant, P. R. L. (2002). *Adv. Mater.*, 14, 99.
- [2] Allard, S., Forster, M., Souharcé, B., Thiem, H., & Scherf, U. (2008). *Angew. Chem. Int. Ed.*, 47, 4070.
- [3] McCulloch, I., Heeney, M., Bailey, C., Gevevicius, K., Macdonald, I., Shkunov, M., Sparrowe, D., Tierney, S., Wagner, R., Zhang, W., Chabiny, M. L., Kline, R. J., McGehee, M. D., & Toney, M. F. (2006). *Nature Mater.*, 5, 328.
- [4] van Breemen, A. J. J. M., Herwig, P. T., Chlon, C. H. T., Sweelssen, J., Schoo, H. F. M., Setayesh, S., Hardeman, W. M., Martin, C. A., de Leeuw, D. M., Valetton, J. J. P., Bastiaansen, C. W. M., Broer, D. J., Popa-Merticaru, A. R., & Meskers, S. C. J. (2006). *J. Am. Chem. Soc.*, 128, 2336.
- [5] Funahashi, M., Zhang, F., & Tamaoki, N. (2007). *Adv. Mater.*, 19, 353.
- [6] Oikawa, K., Monobe, H., Nakayama, K., Kimoto, T., Tsuchiya, K., Heinrich, B., Guillon, D., Shimizu, Y., & Yokoyama, M. (2007). *Adv. Mater.*, 19, 1864.
- [7] Shimizu, Y., Monobe, H., Heinrich, B., Guillon, D., Oikawa, K., & Nakayama, K. (2009). *Mol. Cryst. Liq. Cryst.*, 509, 206.
- [8] Iino, H., & Hanna, J. (2009). *Mol. Cryst. Liq. Cryst.*, 510, 259.
- [9] Chaure, N. B., Pal, C., Barard, S., Kreouzis, T., Ray, A. K., Cammidge, A. N., Chambrier, I., Cook, M. J., Murphyc, C. E., & Cain, M. G. (2012). *J. Mater. Chem.*, 22, 19179.
- [10] Ebata, H., Izawa, T., Miyazaki, E., Takimiya, K., Ikeda, M., Kuwabara, H., & Yui, T. (2007). *J. Am. Chem. Soc.*, 129, 15732.
- [11] Uemura, T., Hirose, Y., Uno, M., Takimiya, K., & Takeya, J. (2009). *Appl. Phys. Express*, 2, 111501.
- [12] Izawa, T., Miyazaki, E., & Takimiya, K. (2008). *Adv. Mater.*, 20, 3388.
- [13] Minemawari, H., Yamada, T., Matsui, H., Tsutsumi, J., Haas, S., Chiba, R., Kumai, R., Hasegawa, T. (2011). *Nature*, 475, 364.
- [14] Liu, C., Minari, T., Lu, X., Kumatani, A., Takimiya, K., & Tsukagoshi, K. (2011). *Adv. Mater.*, 23, 523.
- [15] Nakayama, K., Hirose, Y., Soeda, J., Yoshizumi, M., Uemura, T., Uno, M., Li, W., Kang, M. J., Yamagishi, M., Okada, Y., Miyazaki, E., Nakazawa, Y., Nakao, A., Takimiya, K., & Takeya, J. (2011). *Adv. Mater.*, 23, 1626.
- [16] Soeda, J., Hirose, Y., Yamagishi, M., Nakao, A., Uemura, T., Nakayama, K., Uno, M., Nakazawa, Y., Takimiya, K., & Takeya, J. (2011). *Adv. Mater.*, 23, 3309.
- [17] Iino, H., & Hanna, J. (2011). *J. Appl. Phys.*, 109, 074505.
- [18] Iino, H., & Hanna, J. (2011). *Adv. Mater.*, 23, 1748.
- [19] Amin, A. Y., Reuter, K., Meyer-Friedrichsen, T., & Halik, M. (2011). *Langmuir*, 27, 15340.
- [20] Iino, H., Kobori, T., & Hanna, J. (2012). *Jpn. J. Appl. Phys.*, 51, 11PD02.
- [21] Liu, C., Minari, T., Li, Y., Kumatani, A., Lee, M. V., Pan, A. H. A., Takimiya, K., & Tsukagoshi, K. (2012). *J. Mater. Chem.*, 22, 8462.
- [22] Minari, T., Liu, C., Kano, M., & Tsukagoshi, K. (2012). *Adv. Mater.*, 24, 299.
- [23] Li, Y., Liu, C., Lee, M. V., Xu, Y., Wang, X., Shi, Y., & Tsukagoshi, K. (2013). *J. Mater. Chem. C*, 1, 1352.
- [24] Yuan, Y., Giri, G., Ayzner, A. L., Zoombelt, A. P., Mannsfeld, S. C. B., Chen, J., Nordlund, D., Toney, M. F., Huang, J., & Bao, Z. (2014). *Nature Comm.*, 5, 3005.
- [25] Košata, B., Kozmik, V., Svoboda, J., Novotná, V., Vaněk, P., & Glogarová, M. (2003). *Liq. Cryst.*, 30, 603.
- [26] Park, S. K., Mourey, D. A., Subramanian, S., Anthony, J. E., & Jackson, T. N. (2008). *Appl. Phys. Lett.*, 93, 043301.
- [27] Natali, D., & Caironi, M. (2012). *Adv. Mater.*, 24, 1357.